Supplementary Material for "Transmembrane helices have rough energy surfaces"

by Harald Janovjak, Helene Knaus, and Daniel J. Müller

Materials and Methods

Preparation of native purple membranes

Native purple membranes were extracted from *Halobacterium salinarum*[1] and adsorbed to freshly cleaved mica from buffer solution (300 mM KCl, 20 mM Tris, pH 7.8)[2]. All buffer solutions were prepared with nanopure water and p.a. grade chemicals from Sigma/Merck.

Variable temperature single-molecule force spectroscopy

A commercial AFM (PicoForce MultiMode, Veeco, Santa Barbara, CA) was equipped with silicon nitride (Si_3N_4) cantilevers (NPS from Veeco and OTR-4 from Olympus, Tokyo, Japan). A heater (Veeco Thermoheater) was magnetically mounted between the piezoelectric scanner and the sample. At room temperature we measured a sample temperature of 27°C. For other measurements, the heater was adjusted to 42°C and the sample temperature was controlled with an accuracy of 1°C using a calibrated digital thermometer. Measurements at 18°C were performed by placing the AFM into a custom-made temperature-controlled box. The spring constants of the cantilevers (≈ 0.06 N/m) were calibrated in solution using thermal fluctuation analysis[3] after calibrating the optical sensitivity by pressing on a hard surface. We examined the influence of temperature on the optical sensitivity or spring constant of the cantilever force sensor. Both properties appear to be constant in the studied temperature range for the Si_3N_4 cantilevers used here, while a small change in optical sensitivity was detected for thinner Si_3N_4 cantilevers (≈ 15% per 20°C; Figure 1S). The pH of the buffer (300 mM KCl, 20 mM Tris, pH 7.8) was adjusted at the temperature at which the experiments were performed. Force spectroscopy and data analysis of the 1193 single-molecule force traces were performed as described.[4] At 18°C, we analyzed 14 (87 nm/s), 19 (163 nm/s), 79 (654 nm/s), 77 (1310 nm/s),

and 90 (2620 nm/s) force traces; at room temperature, we analyzed 10 (10 nm/s), 84 (50 nm/s), 79 (87 nm/s), 165 (654 nm/s), 121 (1310 nm/s), 23 (2620 nm/s), and 51 (5230 nm/s) force traces; at 42°C, we analyzed 59 (87 nm/s), 103 (300 nm/s), 101 (654 nm/s), 78 (1310 nm/s), and 40 (5000 nm/s) force traces at the indicated pulling speeds. Room-temperature data were taken from a recent publication.[4] As described earlier, only helices A-E of bacteriorhodopsin are resolved in single-molecule pulling experiments due to non-specific tip-surface interactions.[5]

Dynamic force spectroscopy and calculations of energy landscape roughness

To obtain the width of the potential barriers, x_β, and the natural (force-free) off-rates, k_u, from the dynamic force spectroscopy data we applied Monte-Carlo (MC) simulations[6] and the model of Evans and Ritchie.[7] In latter case, line fits to force vs. loading-rate plots (e.g. Figure 1C) yield slopes corresponding of k_BT/x_β and x-intersections of k_BTk_u/x_β.[7] $x_\beta=cos(\theta)x_u$ represents the thermally averaged projection of the barrier along the direction of force, and the angle θ accounts for deviations of the reaction coordinate from the pulling direction.[7] We estimated the force loading rates using a line-fit[8] to a worm like chain (WLC)-curve of the same contour length as the corresponding force peak. We used 30% of the most probable unfolding force as the lower and the most probable unfolding force as the upper boundary of the fit. MC simulations were performed as recently described[6] and fit to force vs. velocity data using chi-square minimization.[4,9] The Evans model and MC simulations yield similar results (Table 1S).

The estimates of the free energy of activation, ΔG_u^* (Table 2S), were calculated following an Arrhenius equation of the type

$$k_u = \frac{1}{\tau_D} e^{\frac{-\Delta G_u^*}{k_B T}}$$

where τ_D is the diffuse relaxation time. For proteins, typical values of τ_D are of the order of 10^{-7} - 10^{-9} s.[10] Varying τ_D in this range changes the free energy of activation by <10%.

Standard spreadsheet programs are not well suited for calculating the energy surface ruggedness following Eq. 1, since very small numbers occur in its first terms if SI-units (Système International d'Unités) are used. Here Igor Pro (Wavemetrics, Lake Oswego, OR) with 64-bit double-precision variables was used for all calculations.

Tables and Figures

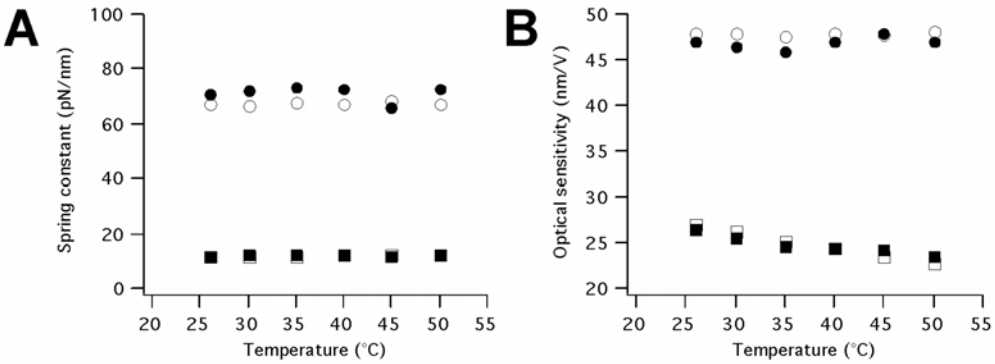

Figure 1S: Spring constant and optical sensitivity as a function of temperature. We examined the influence of temperature on the optical sensitivity and spring constant of different cantilever force sensors (in duplicates). In the studied temperature range, both properties appear to be constant for the Si_3N_4 cantilevers used (circles; NP-S), while a small change in optical sensitivity was detected for two of the thinnest commercially available cantilevers (squares; Biolever B, Olympus, Tokyo, Japan)

Structural Element	Evans model		MC-simulation	
	x_β [Å]	k_u [s^{-1}]	x_β [Å]	k_u [s^{-1}]
Pairwise unfolding of α-helices				
α-helices E&D *	3.55 ± 0.18	4.7 ± 2.6 X 10^{-3}	3.2	1.0 X 10^{-2}
α-helices C&B *	6.52 ± 1.65	7.00 ± 21.4 X 10^{-4}	8.6	3.4 X 10^{-5}
Single secondary structure elements				
α-helix E **	4.44 ± 0.69	2.3 ± 5.3 X 10^{-4}	4.6	1.1 X 10^{-4}
α-helix D	5.92 ± 1.93	1.5 ± 3.6 X 10^{-2}	7.7	1.5 X 10^{-2}
α-helix D	3.59 ± 0.74	1.2 ± 1.6 X 10^{-1}	4.0	5.6 X 10^{-2}
α-helix C	4.31 ± 0.87	2.3 ± 4.2 X 10^{-2}	3.9	5.6 X 10^{-2}
α-helix C	4.71 ± 0.38	8.8 ± 6.8 X 10^{-3}	4.9	6.0 X 10^{-3}
α-helix B	4.80 ± 0.65	6.6 ± 6.9 X 10^{-2}	5.4	3.1 X 10^{-2}
α-helix B	5.45 ± 0.94	1.9 ± 2.8 X 10^{-2}	5.7	1.7 X 10^{-2}
α-helix A ***	6.78 ± 0.97	1.9 ± 3.6 X 10^{-4}	6.8	1.8 X 10^{-4}
Loop BC	6.13 ± 1.79	1.4 ± 4.6 X 10^{-3}	5.8	3.0 X 10^{-3}

* Including the connecting loops
** Including the 3 aa long loop DE
*** Including the 7 aa long N-terminus

Table 1S: Mechanical energy landscapes of transmembrane structures. The widths of the potential barriers, x_β, and unfolding rates, k_u, were obtained using the model of Evans and MC simulations from force vs loading-rate or force vs velocity plots with room-temperature data (see Materials and Methods). Both approaches yield similar results. The results of the MC simulations are taken from Ref. 4.

Structural Element	x_β [Å] 18°C 42°C	k_u [s^{-1}] 18°C 42°C	ΔG_u^* [pN nm] 18°C 42°C
Pairwise unfolding of α-helices			
α-helices E&D *	4.28 ± 1.46 2.67 ± 0.27	1.6 ± 7.8 X 10^{-4} 2.5 ± 0.2 X 10^{-1}	109.16 86.15
α-helices C&B *	7.67 ± 0.03 4.11 ± 0.40	1.2 ± 2.7 X 10^{-5} 8.1 ± 5.6 X 10^{-2}	119.43 91.03
Single secondary structure elements			
α-helix E **	6.16 ± 0.91 4.36 ± 0.62	2.0 ± 6.2 X 10^{-7} 4.7 ± 7.4 X 10^{-3}	135.96 103.47
α-helix D	4.42 ± 0.72 3.42 ± 0.48	4.1 ± 5.6 X 10^{-2} 8.9 ± 6.8 X 10^{-1}	86.85 80.61
α-helix D	3.44 ± 0.72 3.57 ± 0.65	1.2 ± 1.8 X 10^{-1} 2.7 ± 3.4 X 10^{-1}	82.63 85.69
α-helix C	6.48 ± 0.06 4.78 ± 3.07	9.3 ± 2.3 X 10^{-5} 7.8 ± 3.2 X 10^{-2}	111.33 91.24
α-helix C	5.77 ± 0.02 5.17 ± 0.46	2.0 ± 1.3 X 10^{-3} 1.7 ± 1.2 X 10^{-2}	98.93 97.96
α-helix B	4.53 ± 1.5 3.80 ± 0.81	1.6 ± 3.6 X 10^{-1} 1.3 ± 1.3	81.30 78.87
α-helix B	4.55 ± 0.67 4.28 ± 1.38	8.3 ± 8.4 X 10^{-2} 6.3 ± 1.1 X 10^{-1}	84.09 82.10
α-helix A ***	6.63 ± 1.5 7.46 ± 0.005	1.7 ± 5.2 X 10^{-4} 9.2 ± 1.2 X 10^{-4}	108.94 110.52
Loop BC	5.51 ± 1.50 4.43 ± 1.38	1.2 ± 3.1 X 10^{-2} 3.0 ± 8.2 X 10^{-1}	94.10 85.39

* Including the connecting loops
** Including the 3 aa long loop DE
*** Including the 7 aa long N-terminus

Table 2S: Mechanical energy landscapes of transmembrane structures probe at different temperatures. The widths of the potential barriers, x_β, unfolding rates, k_u, and activation energies, ΔG_u^*, of the transmembrane structures were obtained using the model of Evans and an Arrhenius equation at different temperatures (see Materials and Methods).

Structural Element	ε [pN*nm]
Pairwise unfolding of α-helices	
α-helices E&D *	24.63
α-helices C&B *	27.02
Single secondary structure elements	
α-helix E **	22.61
α-helix D	no value[1]
α-helix D	16.52
α-helix C	21.16
α-helix C	24.04
α-helix B	8.33
α-helix B	19.73
α-helix A ***	10.75
Loop BC	22.20
* Including the connecting loops ** Including the 3 aa long loop DE *** Including the 7 aa long N-terminus	

Table 3S: Energy surface roughness does not depend on the temperature range. The energy landscape roughness was re-calculated with dynamic force spectroscopy (DFS) data recorded at 18 and 27°C with a force treshold of 50 pN. For helix D ([1]), only one value could be determined due to a negative term in Eq. 1.

References

(1) Oesterhelt, D.; Stoeckenius, W. *Methods Enzymol* **1974**, *31*, 667-678.

(2) Müller, D. J.; Amrein, M.; Engel, A. *J Struct Biol* **1997**, *119*, 172-188.

(3) Florin, E. L.; Rief, M.; Lehmann, H.; Ludwig, M.; Dornmair, C.; Moy, V. T.; Gaub, H. E. *Biosensors Bioelectr* **1995**, *10*, 895-901; Butt, H. J.; Jaschke, M. *Nanotechnology* **1995**, *6*, 1-7.

(4) Janovjak, H.; Struckmeier, J.; Hubain, M.; Kedrov, A.; Kessler, M.; Müller, D. J. *Structure* **2004**, *12*, 871-879.

(5) Müller, D. J.; Kessler, M.; Oesterhelt, F.; Möller, C.; Oesterhelt, D.; Gaub, H. *Biophys J* **2002**, *83*, 3578-3588.

(6) Rief, M.; Fernandez, J. M.; Gaub, H. E. *PRL* **1998**, *81*, 4764-4767.

(7) Evans, E. *Annu Rev Biophys Biomol Struct* **2001**, *30*, 105-128; Evans, E.; Ritchie, K. *Biophys J* **1997**, *72*, 1541-1555.

(8) Dettmann, W.; Grandbois, M.; Andre, S.; Benoit, M.; Wehle, A. K.; Kaltner, H.; Gabius, H. J.; Gaub, H. E. *Arch Biochem Biophys* **2000**, *383*, 157-170.

(9) Best, R. B.; Fowler, S. B.; Toca-Herrera, J. L.; Clarke, J. *Proc Natl Acad Sci. USA* **2002**, *99*, 12143-12148.

(10) Yang, W. Y.; Gruebele, M. *Nature* **2003**, *423*, 193-197; Lapidus, L. J.; Eaton, W. A.; Hofrichter, J. *Proc Natl Acad Sci U S A* **2000**, *97*, 7220-7225; Bieri, O.; Wirz, J.; Hellrung, B.; Schutkowski, M.; Drewello, M.; Kiefhaber, T. *Proc Natl Acad Sci U S A* **1999**, *96*, 9597-9601.